THE UNIVERSITY *of* EDINBURGH

Edinburgh Research Explorer

Emergence of Molecular Recognition Phenomena in a Simple Model of Imprinted porous Materials

Link:
Link to publication record in Edinburgh Research Explorer

Document Version:
Peer reviewed version

Published In:
Journal of Chemical Physics

OPEN ACCESS

Emergence of molecular recognition phenomena in a simple model of imprinted porous materials

Eduardo M. A. Dourado and Lev Sarkisov[a)]

Institute for Materials of Processes, The University of Edinburgh, King's Buildings,
Mayfield Road, EH9 3JL Edinburgh, United Kingdom

Polymerization in the presence of templates, followed by their consequent removal, leads to structures with cavities capable of molecular recognition. This molecular imprinting technology has been employed to create porous polymers with tailored selectivity for adsorption, chromatographic separations, sensing, and other applications. Performance of these materials crucially depends on the availability of highly selective binding sites. This parameter is a function of a large number of processing conditions and is difficult to control. Furthermore, the nature of molecular recognition processes in these materials is poorly understood to allow a more systematic design. In this work we propose a simple model of molecularly imprinted polymers mimicking the actual process of their formation. We demonstrate that a range of molecular recognition effects emerge in this model and that they are consistent with the experimental observations. The model also provides a wealth of information on how binding sites form and function in the imprinted structures. It demonstrates the capability to assess the role of various processing conditions in the final properties of imprinted materials, and therefore it can be used to provide some qualitative insights on the optimal values of processing parameters. © *2009 American Institute of Physics.* [DOI: 10.1063/1.3140204]

I. INTRODUCTION

Molecular recognition is a process of strong and specific noncovalent binding between a molecule and a substrate. This mechanism is vital for a number of biological processes including enzymatic reactions, defensive mechanisms, and genetic information replication. Recently, however, a technology has been developed to synthesize abiogenic porous structures capable of biomimetic molecular recognition. At the heart of this technology is the molecular imprinting protocol, where self-assembly of the precursors and polymerization of the material take place in the presence of additional template molecules. The templates are subsequently removed leaving in the final structure cavities, or imprints, which are structurally complementary to the template species. These cavities function as selective binding sites, capable of recognition and rebinding of the original template species. The first observation of molecular recognition in abiogenic structures dates back to 1931, when Polyakov[1] prepared sol-gel materials in the presence of benzene, toluene, and xylene and observed a particular affinity of the resulted structures toward the original additives or related ligands. It was hypothesized that the produced silica materials acquired some kind of *steric memory* toward the guest species. However, the true potential of this approach was realized with the first molecularly imprinted polymers (MIPs) prepared in 1970s.[2] In MIP synthesis, the polymerizing mixture consists of cross-linker component, responsible for the structural integrity of the polymer, and functional monomers, which form associations with the functional groups of the template molecule. Thus, in addition to steric effects, the resulting binding site also fea-tures very specific complementary interaction patterns. The basic steps of this technique are shown in Fig. 1. For example, one of the earliest MIPs was prepared using meth-acrylic acid as the functional monomer and ethylene glycol dimethacrylate as the cross-linking monomer, with two small drug molecules, theophylline and diazepam, as the template species.[3] These structures were able to differentiate between close analogs of the template, exhibiting properties similar to the natural antibodies. This demonstrated the remarkable potential of molecular imprinting. Rich polymeric chemistry and a large number of possible building components opened an opportunity to design highly functionalized materials for chromatographic separations, sensing, artificial immunoas-says, catalysis, and other applications implemented over the last 20 years.[2]

Despite these successes, synthesis of MIPs remains an intricate and vastly empirical process.[4] It has been well established in a number of studies that MIPs have few selective binding sites and a large number of relatively nonselective sites.[5] This heterogeneity of binding sites is an intrinsic feature of the imprinting technique. The performance of a MIP crucially depends on this characteristic, and it is important to be able to control it. For this we need a detailed understanding of how specific binding sites form and function.

Recent experimental and theoretical studies suggest that very selective, high quality binding sites result from strong associations between the functional monomers and template species.[6–10] For example, in the aforementioned study by Vlatakis *et al.*,[3] methacrylic acid forms ionic interactions and hydrogen bonds with amino and polar functional groups of the template. Naturally, most of the recent design efforts have been focused on screening for appropriate functional

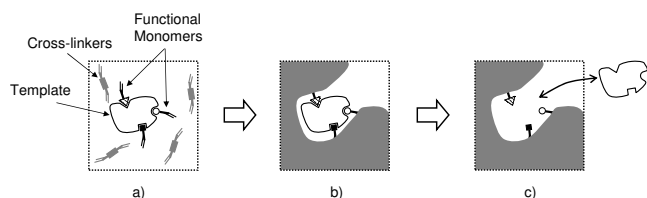[a)]Electronic mail: lev.sarkisov@ed.ac.uk.

FIG. 1. A schematic depiction of the polymer imprinting principles. (a) A mixture of components is equilibrated and functional monomer-template complexes are formed; (b) polymerization stage; (c) after template extraction, a cavity is left capable of rebinding the template.

84 monomers, which would form stable complexes with the
85 template molecule of interest.[11,12] This, however, is only one
86 of many factors that play a role in the final characteristics of
87 a MIP. First of all, not all of the formed complexes become
88 selective binding sites. Some of the complexes may be de-
89 stroyed during the polymerization process, and others may
90 evolve into inaccessible binding sites either because of a
91 trapped template molecule inside or because they become
92 spatially isolated from the remaining porous space during the
93 polymerization. Furthermore, several scenarios are possible
94 where specific and accessible binding sites are not able to
95 perform their rebinding function. For example, during the
96 adsorption or rebinding process, one or more molecules can
97 form associations with the interaction groups of the binding
98 sites in an arrangement different from the original predeces-
99 sor complex. In general, recognition events in a binding site
100 are strongly affected by the state of the neighboring binding
101 sites and pores. All of these factors may contribute to the
102 diminished performance of a MIP and are intimately linked
103 to the various properties of the imprinted material such as
104 density, concentration of the interaction groups on the sur-
105 face, and so on. As a result MIP performance depends not
106 only on the stability of the complexes between functional
107 monomers and templates in the prepolymerization mixture
108 but also on a number of other processing conditions such as
109 relative concentration of the components, choice of solvent,
110 and polymerization temperature. The number of optimization
111 parameters is large, they are not independent of each other
112 and their mutual effects are quite intricate. Clearly, design of
113 MIPs with tailored functionalities requires some rational
114 strategies.
115   Computational methods and theoretical approaches have
116 been playing an increasingly important role in the develop-
117 ment of these strategies with a number of fundamental mod-
118 els of MIPs recently proposed.[13–16] For example, Yungerman
119 and Srebnik[15] considered a model of a polymerizing
120 Lennard-Jones fluid templated with rigid dimers, also made
121 of two Lennard-Jones sites. Polymerization was modeled as
122 the formation of harmonic bonds between the particles rep-
123 resenting monomers. This model allowed the authors to in-
124 vestigate porosity and pore size distribution in the final struc-
125 ture as function of the template concentration and degree of
126 polymerization. Wu et al.[16] recently proposed a simple two
127 dimensional square lattice model of MIPs. In the model each
128 lattice site can be either empty or occupied by a cross-linker,
129 functional monomer, or template species. Each functional
130 monomer can form an association with only one out of four
131 adjacent lattice sites. Template sites can have up to four

132 monomers associated with it. This leads to binding sites of
133 different types and quality, depending on the number of
134 monomers associated with the site. This model is clearly well
135 suited to explore binding site distributions in MIPs and how
136 this characteristic depends on the relative concentrations of
137 the template and monomer species and on the strength of the
138 template-functional monomer association. It was also applied
139 to a specific case of enantioselective recognition of racemic
140 components. It is also important to note that a number of
141 atomistic models of MIPs have started to emerge
142 recently.[17–26]
143   In this work, we aim to develop a more general, compu-
144 tationally efficient model, which would satisfy the following
145 criteria. The model should reflect the process of MIP forma-
146 tion and feature complex interconnected three dimensional
147 porous space characteristic for MIPs. The model should ex-
148 hibit molecular recognition and provide a tool to investigate
149 the relation between various processing conditions (such as
150 relative concentration of species), porous morphology, and
151 the binding site distribution. Several elements of this strategy
152 have been already developed. Van Tassel et al.[27–31] proposed
153 a series of models, where all species were represented as
154 hard spheres or Lennard-Jones particles. The first step of the
155 model involves an equilibrated mixture of template and ma-
156 trix components (matrix here and throughout the article is a
157 generic term for the polymer components). The mixture is
158 then quenched and the template particles are removed. The
159 resulting structure of the quenched matrix component serves
160 as the model porous material. The advantage of the model is
161 that it also allows for a theoretical treatment within the rep-
162 lica Ornstein–Zernike formalism. It has been shown that the
163 presence of a template enhances adsorption and that the mag-
164 nitude of the effect strongly depends on the template/matrix
165 composition ratio and on the size of the template. However,
166 as expected, no molecular recognition effect could be cap-
167 tured in a system of simple particles. Recently, the model of
168 Van Tassel et al. was extended to molecular species.[32–34] Us-
169 ing both computer simulations and integral equation ap-
170 proaches, a range of systems with either purely repulsive or
171 more complex patterns of interaction was considered. The
172 adsorption of rigid linear chains, clusters, and molecules of
173 other shapes in matrices templated with these species was
174 investigated and a number of nontrivial effects were ob-
175 served. Molecular recognition was also observed for systems
176 interacting with Lennard-Jones-like potentials; however, this
177 observation was limited to one specific system in a narrow
178 range of conditions and therefore it lacks generality.[32]

II. METHODOLOGY

A. Computational strategy

181   In the first step a mixture of the MIP components (tem-
182 plate, cross-linker, and functional monomer) is equilibrated
183 under specified conditions. When equilibrium is reached, the
184 system is quenched (i.e., molecules are frozen in their posi-
185 tions and orientations), this stage imitates polymerization in
186 the actual MIP synthesis. The porous structure formed by the
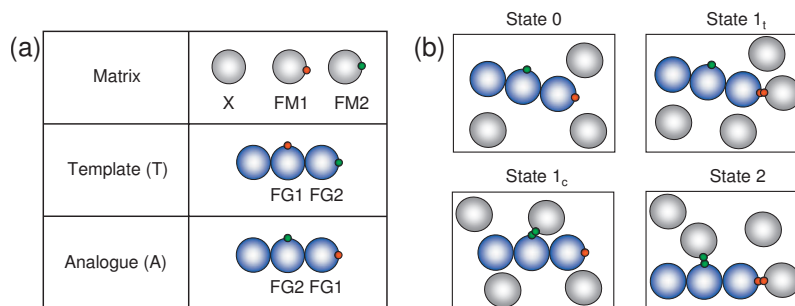187 quenched configurations of the matrix species (cross-linkers

FIG. 2. (Color) (a) Summary of the species considered in this work. Matrix species include cross-linker X and functional monomers FM1 and FM2, which feature surface interaction sites shown in red (FM1) and green (FM2); template (T) is a rigid chain of three tangent hard spheres with surface interaction sites in the arrangement as shown. Functional group FG1 (red interaction site) can associate with functional monomer FM1, functional group FG2 (green interaction site) can associate with functional monomer FM2. Analog A has the location of the functional groups exchanged. (b) Schematic depiction of the possible complexes between the template and functional monomers in the prepolymerization mixture. Each complex is described by the number of associations formed between the template and functional monomers (states 0, 1_t, 1_c, 2), with subscripts t and c signifying the terminal and central location of the engaged functional group, respectively.

188 and functional monomers) models the MIP after template
189 extraction. This simulated MIP is then used in the adsorption
190 simulations.

B. Molecular model

192   In a series of earlier studies, Sarkisov and Van Tassel[32,33]
193 applied the strategy described above to a range of systems
194 where rigid molecules were constructed from a basic build-
195 ing block, such as a hard sphere or a Lennard-Jones-like
196 particle. For example, the template could be represented as a
197 rigid chain of several hard spheres, whereas the polymer was
198 represented simply as a fluid of hard spheres.

199   In order to capture the molecular recognition phenom-
200 ena, we need to go beyond these types of interactions. In
201 experiments, formation of the very specific binding sites re-
202 sults from strong associations between the template molecule
203 and functional monomers. The nature of these associations is
204 complex and includes both hydrogen bonds and electrostatic
205 contributions. To a significant extent, molecular recognition
206 is a process of reforming of these associations in the binding
207 site. Thus, the idea of this work is to extend the model of
208 Sarkisov and Van Tassel to incorporate a simple description
209 of associations forming between functional monomers and a
210 template molecule. The inspiration for our approach comes
211 from an earlier model of water proposed by Kolafa *et al.*[35,36]
212 In their model, water is represented as a hard sphere deco-
213 rated with four additional interaction sites in a tetrahedral
214 arrangement. These interaction sites, located close to or at
215 the surface of the hard sphere, are small compared to the
216 central hard sphere particle and are able to associate with
217 each other via a short range square-well potential. Associa-
218 tions between water particles in this description feature
219 directionality, short range, and strength of hydrogen bonds.
220 Using this approach we construct the species involved in our
221 model as shown in Fig. 2(a). In this study, a cross-linker
222 molecule is a hard sphere of size σ (species X). A functional
223 monomer in this model is represented as a hard sphere of
224 size σ with an interaction site on the surface as shown in Fig.
225 2(a). We consider functional monomers of two types, FM1
226 and FM2, but the model is not limited to this specific case. A
227 template molecule (species T) is a rigid linear chain of three

228 tangent hard spheres of the same size σ. Two of these
229 spheres also feature surface interaction sites in the arrange-
230 ment as shown in Fig. 2(a) and can be viewed as functional
231 groups (FG1 and FG2). Functional monomer FM1 can asso-
232 ciate with functional group FG1, whereas functional mono-
233 mer FM2 can associate with functional group FG2. The as-
234 sociation between interaction sites is modeled via a square-
235 well potential of the following form:

$$u(r)/k_BT = \begin{cases} -\varepsilon/k_BT, & r \le \sigma_{\text{SW}} \\ 0, & r > \sigma_{\text{SW}}, \end{cases} \tag{1}$$

237 where $u(r)$ is the interaction energy between two interaction
238 sites, r is the distance between the two sites, ε determines the
239 well depth of the potential and is equal to $10k_BT$ (typical
240 magnitude for hydrogen bonds), σ_{SW} is the size of the
241 interaction site and is equal to 0.15σ, and k_B and T are the
242 Boltzmann constant and temperature as usual. No functional
243 monomers can associate with each other, and the same is true
244 for the functional groups.

245   One of the key objectives of this study is to test whether
246 the proposed model is capable of molecular recognition. This
247 function would manifest itself in the ability of the model
248 imprinted matrix to preferentially adsorb the original tem-
249 plate species and distinguish them from analogous species
250 that have similar structure and composition but different ar-
251 rangements of the functional groups. An example of such an
252 analog, where the location of the functional groups is ex-
253 changed, is also shown in Fig. 2(a).

C. Characterization of prepolymerization complexes and binding sites

256   In the model presented here, associations form between
257 the functional monomers and the functional groups of the
258 template. In the prepolymerization mixture composed from
259 the species presented in Fig. 2(a), a template molecule can be
260 observed in one of four possible states. These states are
261 shown in Fig. 2(b). In the first state, labeled 0, the template
262 molecule does not form any associations. States (or com-
263 plexes) 1_t and 1_c are characterized by a single association
264 with either the terminal or the central functional group of the
265 template engaged in the association, respectively. (We

266 choose this notation, instead of using FG1 and FG2, since
267 the location of these groups in the template and analog mol-
268 ecules is swapped.) Finally, the template can have associa-
269 tions established with both functional groups and this corre-
270 sponds to state (or complex of type) 2. Computer simulations
271 allow us to monitor the population of these complexes during
272 the equilibration of the matrix and relate these characteristics
273 to various parameters of the system, such as composition and
274 density. Once the system is quenched (imitating polymeriza-
275 tion), the complexes are frozen in their instant configura-
276 tions. Template removal transforms these complexes into
277 binding sites.

278   Let us consider behavior of these binding sites during an
279 adsorption process, where we use template as the adsorbate.
280 Again, adsorbed molecules can be observed in different
281 states, similar to those depicted in Fig. 2(b), depending on
282 the number of associations they form with the matrix. It is
283 important to recognize that not all of these states correspond
284 to molecules located in the binding sites formed during the
285 imprinting. For example, a situation is possible where an
286 adsorbing molecule is able to form two associations with the
287 matrix in an arrangement that does not correspond to any
288 particular complex in the prepolymerization mixture. Thus,
289 to distinguish the states of the adsorbed molecules from
290 those in the prepolymerization mixture, we introduce a clas-
291 sification of adsorbed states similar to that in Fig. 2(b) and
292 based simply on the number of associations the adsorbed
293 molecule forms with the matrix. Specifically, molecules that
294 form two associations with the matrix are denoted as state 2^a
295 ("a" stands here for an adsorbed molecule here); a molecule
296 with only one association made by the terminal functional
297 group is in state 1_t^a; a molecule with only one association
298 made by the central functional group is in state 1_c^a; finally a
299 molecule with no associations is classified as state 0^a. It is
300 instructive to know how many of the molecules in state 2^a
301 are actually located in the binding sites resulted from the
302 complexes of type 2 in the prepolymerization mixture. Com-
303 puter simulations allow us, given a particular state on the
304 adsorption isotherm, to examine the binding state of each
305 molecule.

D. Simulation details

307   The first stage of the proposed computational strategy
308 considers an equilibrium mixture of the template, functional
309 monomer, and cross-linker components. Equilibration of the
310 system is performed in the canonical *NVT* ensemble using
311 the classical Metropolis sampling protocol. The number of
312 canonical Monte Carlo steps (translations and rotations) re-
313 quired for the equilibration is between 3×10^8 and 6×10^8
314 (depending on the system), of these approximately 5×10^7
315 are used to generate average properties of the system. For
316 each system, a total of three different matrix realizations are
317 generated.

318   Simulations of adsorption are performed using the grand
319 canonical Monte Carlo. In this ensemble, temperature T, vol-
320 ume of the system V, and the chemical potential μ/k_BT of
321 the adsorbing species are specified. A point on the adsorption
322 isotherm corresponds to a simulation with approximately 10^8

323 steps performed, with each step being either an insertion,
324 deletion, translation, or rotation attempt. Translations and ro-
325 tations are accepted with the acceptance probability,

$$P_{\text{trans,rot}} = \min(1, e^{-\beta[U_{\text{new}} - U_{\text{old}}]}), \qquad (2)$$

327 where $\beta = 1/k_BT$, U_{old}, and U_{new} are the configurational en-
328 ergies of the system before and after the attempted move,
329 respectively. To increase the efficiency of insertion and dele-
330 tion moves, we implement a volume biased sampling method
331 as described by Snurr *et al.*[37] in the context of adsorption in
332 zeolites. In this method the system is divided into small
333 cubelets. A probe hard sphere particle is placed in the center
334 of each cubelet and tested for overlaps with the particles of
335 the structure. If no overlaps are registered, this cubelet is
336 saved in a list of accessible cubelets. Insertions are then per-
337 formed by random selection of a cubelet from the list. A
338 molecule of adsorbate is randomly placed within the selected
339 cubelet, with this move accepted or rejected based on the
340 following biased probability criterion:

$$P_{\text{ins}} = \min\left(1, \frac{q^{\text{rot}} e^{\beta\mu} V_C}{(N+1)\Lambda^3}\right), \qquad (3)$$

342 where N is the number of adsorbate molecules in the system
343 and V_C is the total volume of all accessible cubelets. Note
344 that the de Broglie wavelength Λ and the ideal gas rotational
345 partition function q^{rot} are implicitly set to σ and 1, respec-
346 tively. In order to preserve the microscopic reversibility, the
347 acceptance criterion for particle deletions also has to be bi-
348 ased,

$$P_{\text{del}} = \min\left(1, \frac{N\Lambda^3}{q^{\text{rot}} e^{\beta\mu} V_C}\right). \qquad (4)$$

350 These simulations are carried out for a range of increasing
351 values of chemical potential. The adsorbed density of the
352 species as a function of the chemical potential constitutes an
353 adsorption isotherm.

III. RESULTS

355   In this study, we explore six different MIP systems and
356 their parameters are given in Table I. MIP1 has characteris-
357 tics, such as the overall density, similar to those in the earlier
358 studies of Sarkisov and Van Tassel.[33] This system features
359 2400 cross-linker particles and 400 functional monomer par-
360 ticles of each type. The system is imprinted with 400 tem-
361 plate molecules. Therefore, the ratio of functional monomers
362 $(N_{\text{FM1}} + N_{\text{FM2}})$ and functional groups $(N_{\text{FG1}} + N_{\text{FG2}})$ is stoichi-
363 ometric in the system. The prepolymerization mixture is
364 placed in a cubic box of 20σ in size. The overall reduced
365 density of the system, $\rho^* = (N_{\text{total}}/V)\sigma^3$, is 0.55 (here N_{total}
366 $= N_X + N_{\text{FM1}} + N_{\text{FM2}} + 3N_T$ is the total number of hard sphere
367 particles present in the system, N_X and N_T is the number of
368 cross-linker and template particles, V is the volume of the
369 system).

370   The first step of the proposed protocol involves simula-
371 tion of an equilibrium mixture of the cross-linker, functional
372 monomers, and template components. Figure 3 summarizes
373 the distribution of complexes observed in this prepolymer-
374 ization mixture. About 25% of templates are able to form

TABLE I. Summary of the compositions and densities $\rho^*=(N_{total}/V)\sigma^3$ for the systems studied in this work. Here, N_{total} is the total number of hard sphere sites in the system, whereas N_X, N_{FM1}, N_{FM2}, and N_T are the number of cross-linker X, functional monomer FM1, functional monomer FM2, and template T particles, respectively.

MIP	N_X	N_{FM1}	N_{FM2}	N_T	ρ^*
1	2400	400	400	400	0.5500
2	1800	300	300	300	0.4125
3	3000	500	500	500	0.6875
4	2800	200	200	400	0.5500
5	1600	800	800	400	0.5500
6	0	1600	1600	400	0.5500

375 associations with two functional monomers. Other states of
376 the template molecules (bound to just one monomer, either
377 FM1 or FM2, or not bound to any functional monomers) are
378 also observed with roughly the same probability of 25% for
379 each state. The final configuration of this mixture is saved,
380 the template species are removed, and the resulting structure
381 represents a model MIP. The most intriguing aspect of this
382 study is to establish whether this model material is capable
383 of molecular recognition. For this we perform single compo-
384 nent adsorption simulations of the template and analog. The
385 analog, as depicted in Fig. 2(a), features exactly the same
386 building blocks and the overall geometry as the template,
387 however, the location of the interaction sites is reversed,
388 compared to the template. Thus, higher adsorbed density of
389 the template compared to the analog at the same correspond-
390 ing chemical potential would signify molecular recognition
391 in the model MIP. Figure 4(a) shows adsorption isotherms
392 for the template and analog. Indeed, adsorption densities for
393 the template are higher throughout the whole range of chemi-
394 cal potentials. A more intuitive way to characterize selectiv-
395 ity of a MIP is the separation factor S, which is the ratio of
396 the adsorbed template and analog densities at the same
397 chemical potential. This factor is plotted in Fig. 4(b). For the
398 whole range of chemical potential, this factor is greater than
399 1, signifying the preferential adsorption of the template com-
400 pared to the analog. As expected, this factor is decreasing at
401 higher loadings, as the highly specific binding sites become
402 occupied at lower chemical potentials and the remaining po-
403 rous space does not exhibit any preferential adsorption. This
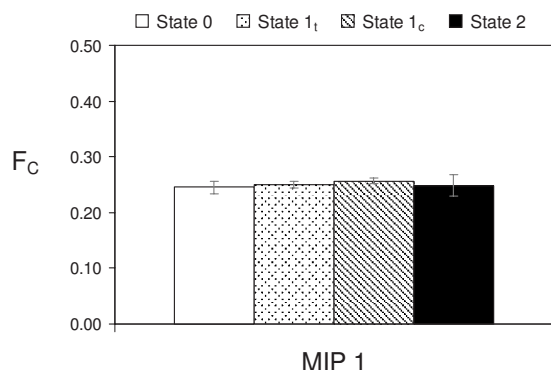404 trend is very similar to what is typically observed in experi-

405 ments, and even the values of the separation factor are com-
406 parable to the typical experimental values in MIP studies.[5]
407 Hence, we establish that the presented model is able to cap-
408 ture molecular recognition effect. Computer simulations al-
409 low us to generate a detailed look at the state of each ad-
410 sorbed molecule and its environment throughout the whole
411 adsorption process. Specifically, for each state on the adsorp-
412 tion isotherm, we have complete information about how
413 many molecules form two associations with the matrix, just
414 one association with the matrix, or have no associations
415 formed at all. Figure 5(a) summarizes the distribution of ad-
416 sorbed molecules among different states of association along
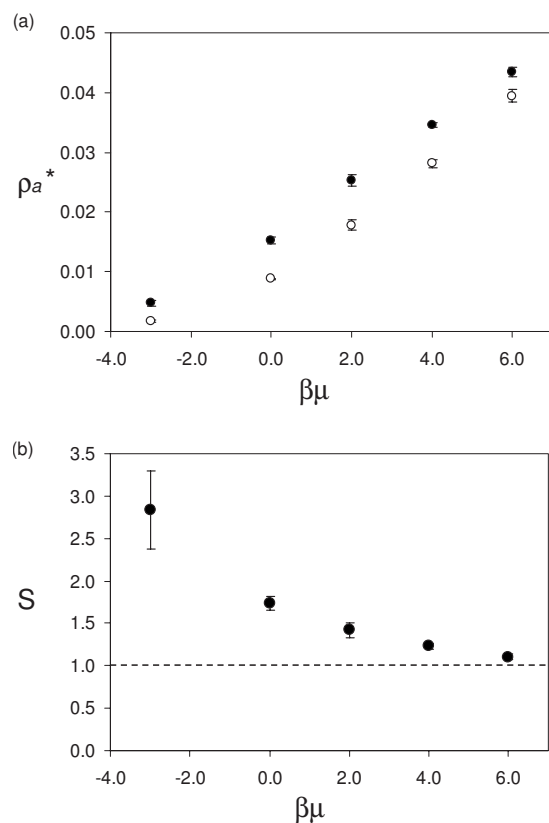417 the adsorption isotherm for MIP1. For example, at the

(a)

(b)

FIG. 4. (a) The adsorption isotherms for MIP1, adsorbate density $\rho_a^*=(N_a/V)\sigma^3$ as a function of the adsorbate chemical potential $\beta\mu$. N_a is the number of adsorbed molecules. Closed symbols correspond to the adsorbed template density $\rho_{a,T}^*$ and open symbols correspond to the adsorbed analog density $\rho_{a,A}^*$. (b) Separation factor $S=\rho_{a,T}^*/\rho_{a,A}^*$ as a function of the chemical potential $\beta\mu$ for MIP1.
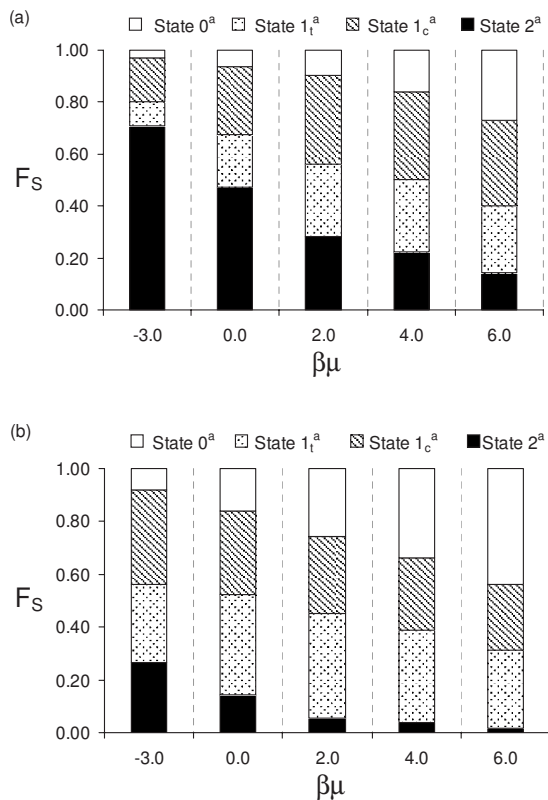

□ State 0   ▨ State 1_t ▨ State 1_c ■ State 2

MIP 1

FIG. 3. Equilibrium distribution of the template-functional monomer complexes in MIP1 system prior to polymerization. F_C is the fraction of complexes of each type.

(a)

(b)

FIG. 5. Fraction F_S of adsorbed molecules in each binding state as a function of the chemical potential $\beta\mu$ in MIP1 for the template (a) and analog (b).
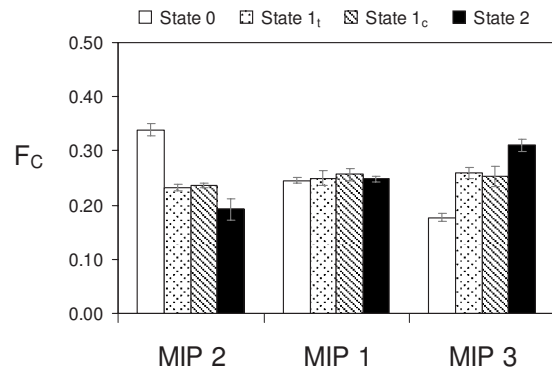

FIG. 6. Equilibrium distribution of the template-functional monomer complexes in MIP2 and MIP3 systems prior to polymerization, compared to this distribution in MIP1. F_C is the fraction of complexes of each type.

418 chemical potential $\beta\mu = -3.0$, there are about 70% of ad-
419 sorbed molecules in 2^a state, 9% in 1_t^a state, 18% in 1_c^a state,
420 and 3% not forming any associations (state 0). Overall, at
421 lower values of the chemical potential, the majority of the
422 adsorbed molecules form two associations with the matrix.
423 As the loading of the material increases, progressively more
424 and more molecules are able to form only one association
425 with the matrix or no associations at all. Interestingly, at the
426 highest loading the distribution of binding sites among dif-
427 ferent association states resembles the distribution of com-
428 plexes in the prepolymerization mixture. It is also instructive
429 to apply similar analysis to the analog adsorption in the same
430 material. Figure 5(b) shows distribution of adsorbed mol-
431 ecules among different binding states for the analog in MIP1.
432 The most important feature of this result is a significant frac-
433 tion of analog molecules that are able to form two associa-
434 tions with the matrix despite the porous space being specifi-
435 cally tailored to recognize the interaction pattern of the
436 template.
437   In order to investigate the effect of density on molecular
438 recognition in MIPs, we consider two variations of MIP1.
439 Both of the systems feature the same mole fractions of the
440 components as MIP1; however, MIP2 has lower overall den-
441 sity than MIP1 (75% of MIP1) and MIP3 has higher overall
442 density than MIP1 (125% of MIP1). It is important to note,
443 that as we increase the density of the material, some of the
444 binding sites may become inaccessible; however, at this
445 stage we do not address this issue. Analysis of the prepoly-
446 merization states of these systems as shown in Fig. 6, reveals
447 that higher density leads to a noticeably higher proportion of

type 2 complexes observed in the mixture. High density of **448**
the mixture also induces stronger complementarity between **449**
the template and the resulting binding site. All these factors **450**
lead to higher selectivity in MIP3 compared to the materials **451**
of lower density. Figure 7 summarizes adsorption isotherms **452**
and separation factors for all three materials. Although, ca- **453**
pacity of MIP3 is lower compared to other materials due to **454**
the reduced porosity, this system exhibits significantly higher **455**
separation factors reaching more than 7 at the lowest value of **456**
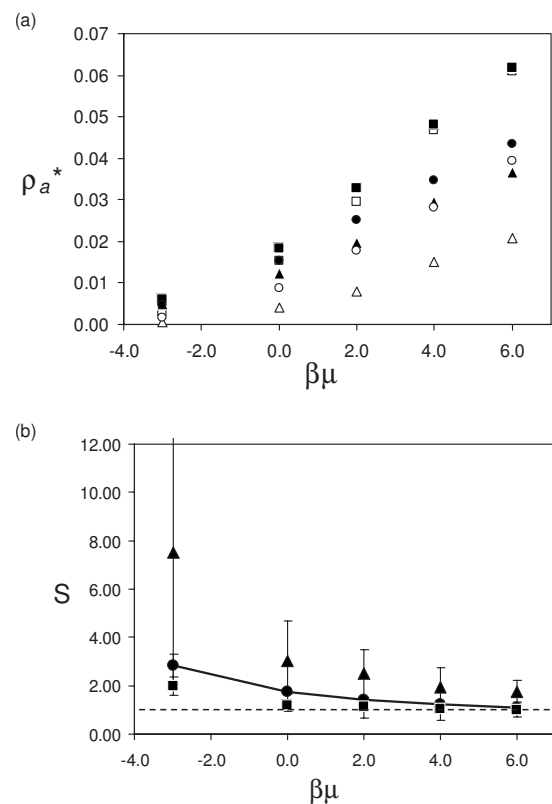the chemical potential shown in the figure. **457**

(a)

(b)

FIG. 7. (a) The adsorption isotherms for MIP1 (circles), MIP2 (squares), and MIP3 (triangles), adsorbate density $\rho_a^* = (N_a/V)\sigma^3$ as a function of the adsorbate chemical potential $\beta\mu$. N_a is the number of adsorbed molecules. Closed symbols correspond to the adsorbed template density $\rho_{a,T}^*$ and open symbols correspond to the adsorbed analog density $\rho_{a,A}^*$. Error bars are not shown for clarity. (b) Separation factor $S = \rho_{a,T}^*/\rho_{a,A}^*$ as a function of chemical potential $\beta\mu$ for MIP1 (circles and solid line), MIP2 (squares), and MIP3 (triangles).
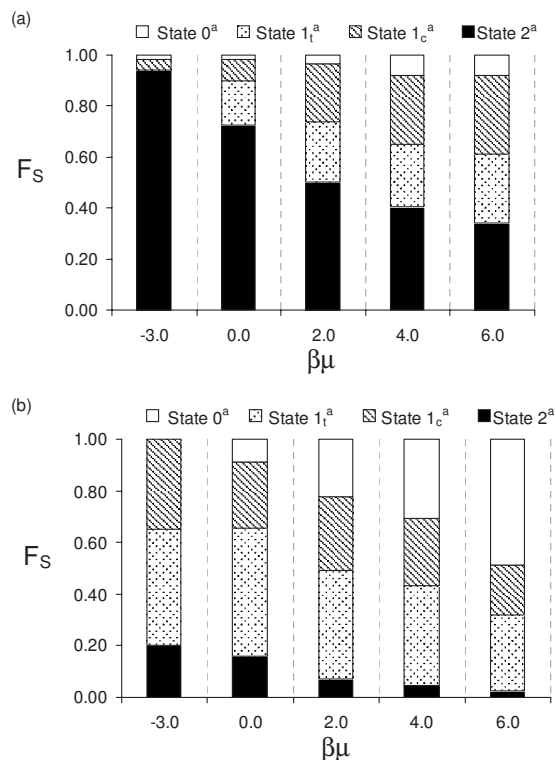
(a)

(b)

FIG. 8. Fraction F_S of adsorbed molecules in each binding state as a function of the chemical potential $\beta\mu$ in MIP3 for the template (a) and analog (b).
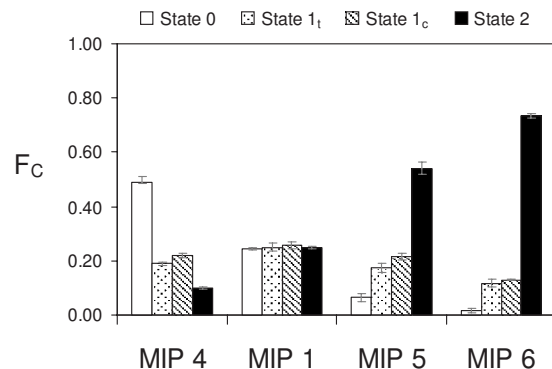

FIG. 9. Equilibrium distribution of the template-functional monomer complexes in MIP4, MIP5, and MIP6 systems prior to polymerization, compared to this distribution in MIP1.

458   We perform analysis of the states of the template and
459 analog molecules adsorbed at each point on the isotherm and
460 observe that for MIP3 templates are predominantly adsorbed
461 in type 2^a states for a significant part of the isotherm (Fig. 8).
462 Although, some analogs also appear to be bound in type 2^a
463 state, the fraction of these is relatively small throughout the
464 isotherm. Thus, higher density leads to more specific binding
465 sites and more pronounced molecular recognition.

466   Composition of the prepolymerization mixture is also a
467 crucial optimization parameter. Both relative amounts of
468 cross-linker and functional monomer (X:M ratio) and func-
469 tional monomer and template (M:T ratio) are important and
470 are not independent from each other. It has been observed in
471 a number of studies that selectivity of MIPs goes through a
472 maximum as these ratios are varied in a systematic way (for
473 a comprehensive review of these effects, we recommend a
474 recent article by Spivak[38]). Here we study the effect of X:M
475 ratio by changing the relative amounts of cross-linker and
476 functional monomer, while maintaining the overall density of
477 the system and the amount of the template constant. (Here
478 $X=N_X$, $M=N_{FM1}+N_{FM2}$). We change the number of func-
479 tional monomers simply by turning the cross-linker particles
480 into functional monomers as required. The reference MIP1
481 has a 3:1 ratio of cross-linker to functional monomer. Three
482 variations on this ratio are explored. MIP4 features lower
483 number of functional monomers (X:M ratio of 7:1), MIP5
484 has double the number of functional monomers (X:M ratio of
485 1:1), and MIP6 has quadruple the number of functional
486 monomers (X:M ratio of 0:1) compared to MIP1. Prepoly-
487 merization mixture of MIP6 consists of functional monomers
488 and templates only, with no cross-linker particles. Therefore,

we investigate a range of regimes from the one correspond- 489
ing to the deficit of functional monomers (MIP4) to the other 490
extreme where the whole polymer is constructed solely from 491
the functional monomer (MIP6). As we increase the number 492
of functional monomers in the system, the fraction of type 2 493
complexes also increases and this is shown in Fig. 9. In 494
MIP6, for example, almost 75% of template molecules are in 495
state 2 in the prepolymerization mixture. Furthermore, at a 496
given value of the chemical potential, the selectivity of ma- 497
terials goes through a maximum, with MIP5, corresponding 498
to X:M ratio of 1:1, exhibiting the highest selectivity. Figure 499
10 summarizes this behavior for three different values of the 500
chemical potential. This behavior is particularly pronounced 501
at the lower values of the chemical potential where adsorp- 502
tion takes place predominantly in very selective binding 503
sites. The explanation of this maximum in selectivity is as 504
follows. At a low concentration of the functional monomer, 505
there are simply not enough functional monomers to form 506
complexes of type 2 with all the available templates. As this 507
concentration is increased, the equilibrium is shifted toward 508
formation of type 2 complexes, leading to a larger number of 509
highly specific 2^a binding sites. However, in the other ex- 510
treme situation abundance of functional monomers leads not 511
only to a larger number of type 2 complexes but also to a 512
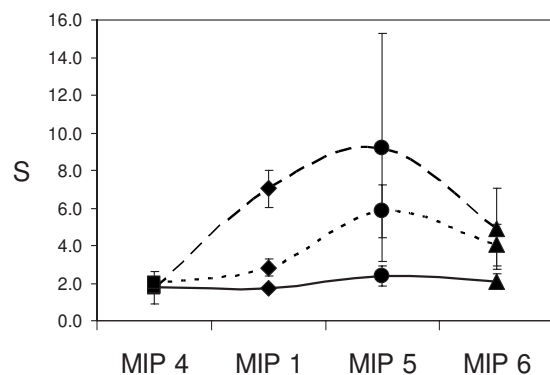significant number of free functional monomers. Therefore, 513

FIG. 10. Selectivity of model MIP structures as a function of cross-linker to functional monomer (X:M) ratio. From left to right: MIP4 X:M=7:1 (squares), MIP1 X:M=3:1 (diamonds), MIP5 X:M=1:1 (circles), and MIP6 X:M=0:1 (triangles). The data are plotted at three different values of the chemical potential $\beta\mu=-5.0$ (broad-dashed line), $\beta\mu=-3.0$ (dashed line), and $\beta\mu=0.0$ (solid line).
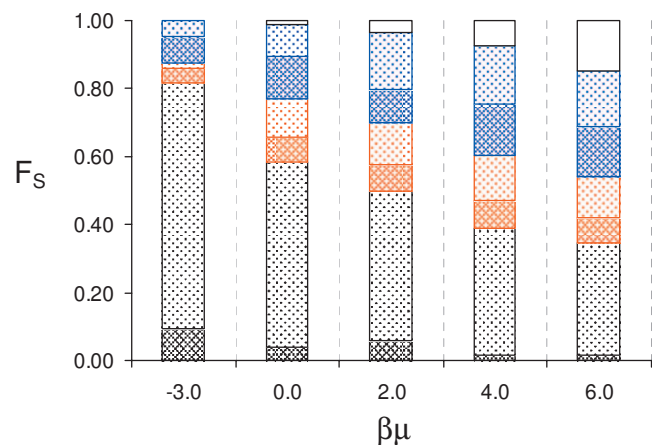
FIG. 11. (Color) Fraction F_S of adsorbed template molecules in each binding state as a function of the chemical potential $\beta\mu$ in MIP5. Color of each bar corresponds to a particular adsorbed state: gray for 2^a, blue for 1_c^a, red for 1_t^a, and white for 0^a states, respectively. Lighter shades correspond to molecules located in the binding sites, formed from the prepolymerization complexes. Darker shades correspond to molecules forming alternative associations with the matrix.

514 additional opportunities open for the analog to form two as-
515 sociations (state 2^a) upon adsorption. This limits the effect of
516 the imprinting on the structure and the resulting MIP exhibits
517 less specific binding.
518   It is also interesting to examine the nature of binding
519 states of adsorbed molecules in the imprinted materials. Spe-
520 cifically, we would like to assess how many molecules in a
521 particular state are actually located in the binding sites
522 evolved from the corresponding complexes in the prepoly-
523 merization mixture. For this, in Fig. 11, we consider the most
524 selective material MIP5 and, in addition to the original dis-
525 tribution of adsorbed molecules among various binding
526 states, we also delineate between *rebinding* to the original
527 binding sites (lighter patterns) and forming new associations,
528 not observed during the prepolymerization (darker patterns).
529 For example, at the chemical potential $\beta\mu=-3.0$ about 81%
530 of all adsorbed molecules are in 2^a state (gray patterns), but
531 about 9% are in 2^a binding sites that did not form from type
532 2 complexes during the imprinting process. About 5% of
533 molecules are in state 1_t^a (red patterns), but only 1% are in
534 the binding sites formed from 1_t complexes, and about 14%
535 of adsorbed molecules are in 1_c^a state (blue patterns), but only
536 4% are located in the binding sites formed from 1_c com-
537 plexes. This analysis indicates that about 10% of the most
538 specific binding sites identified from a typical binding site
539 distribution method, such as the Freundlich isotherms, may
540 not have originated from imprinting.

IV. CONCLUSIONS

542   In this article we propose a simple model of imprinted
543 porous materials. For the first time, molecular recognition
544 effect emerges in the model of MIPs. Molecular species in
545 this model are treated as either hard spheres or rigid clusters
546 of hard spheres. Some of the hard spheres also feature small
547 interaction sites capable of associating with each other in a
548 prescribed manner. These associations aim to imitate interac-
549 tions between the functional monomers and functional

550 groups in real MIPs and prove to be crucial for molecular
551 recognition to emerge in the model. Our previous models
552 based on simpler, less specific interactions were insufficient
553 to capture this effect.
554   At the heart of the model is the general simulation pro-
555 tocol aimed to closely mimic various stages of MIP forma-
556 tion and function. Equilibration of the prepolymerization
557 mixture of components followed by quenching of the mix-
558 ture and removal of the template leads to realistic imprinted
559 structures featuring complex interconnected porous space.
560 Thus, this approach makes it possible to explore all elements
561 relevant to MIP performance, such as molecular recognition
562 effects, binding sites structure, heterogeneity and distribu-
563 tion, pore size distribution, and connectivity within the
564 framework of a single model. This realism of the model en-
565 sures that it is able to capture a number of experimentally
566 observed trends. Specifically, it generates realistic values of
567 separation factors that diminish with increased loading in
568 accordance with experimental observations. Furthermore, the
569 model predicts that with higher density of the material the
570 quality of imprinting improves, leading to more specific
571 binding sites, and hence, higher selectivity of the model MIP.
572 We briefly explored predictions of the model for other pro-
573 cessing conditions such as the ratio of cross-linker to func-
574 tional monomer in the prepolymerization mixture. The model
575 predicts a maximum in the selectivity of model materials, as
576 this ratio is varied. At low concentration of the functional
577 monomers, there is simply not enough monomers to form
578 complexes with all available templates. On the other hand,
579 very high concentrations of the functional monomer result in
580 predominantly nonspecific binding. This is in agreement with
581 experimental observations, although an additional factor no-
582 ticed in experiments is lower rigidity and robustness of the
583 polymer network at high concentrations of the functional
584 monomer.[39] In general, this is an encouraging result as the
585 model demonstrates the capability to assess the role of vari-
586 ous processing conditions in the final properties of MIPs, and
587 therefore it can be used to provide some qualitative insights
588 on the optimal values of processing parameters.
589   We expect that the model can make a particular impor-
590 tant contribution to our understanding of molecular recogni-
591 tion mechanisms in MIPs. In the range of conditions ex-
592 plored in this work, we consistently observe that the analog
593 molecules are able to form very favorable associations with
594 the matrix even though the porous space is imprinted to rec-
595 ognize the interaction pattern of the template. This is an im-
596 portant contribution to a diminished selectivity of MIPs,
597 highlighted by this model.
598   Several aspects of the model require further develop-
599 ment. In the current version the polymerization process is
600 modeled simply by quenching molecules of the prepolymer-
601 ization mixture in their instant locations and orientations. A
602 more realistic approach would involve some mechanism of
603 association between cross-linkers and functional monomers.
604 This model would be able to generate connected and self-
605 sustaining polymer networks. This can be easily imple-
606 mented using the same language of surface interaction sites
607 that we use to describe functional monomer–functional
608 group associations. Furthermore, in this study we do not ad-

dress the accessibility of the binding sites, and this is an important factor to be investigated in our future work. It is also important to explore molecular recognition effects as a function of molecular geometry. Our preliminary studies on the systems with a single type of functional monomer and a single functional group (the analog then differs from the template by the location of the functional group) suggest that the main conclusions of this work remain valid for this simpler case; however, the magnitude of the observed separation factors is lower. Therefore, the main focus of the future work will be on more complex systems, where one might expect a richer spectrum of behavior.

ACKNOWLEDGMENTS

[1] ■ Polyakov, Zh. Fiz. Khim. ■, 799 (1931).
[2] C. Alexander, H. S. Andersson, L. I. Andersson, R. J. Ansell, N. Kirsch, I. A. Nicholls, J. O'Mahony, and M. J. Whitcombe, J. Mol. Recognit. **19**, 106 (2006).
[3] G. Vlatakis, L. I. Andersson, R. Müller, and K. Mosbach, Nature (London) **361**, 645 (1993).
[4] P. A. G. Cormack and A. Z. Elorza, J. Chromatogr. B Analyt. Technol. Biomed. Life Sci. **804**, 173 (2004).
[5] R. J. Umpleby, S. C. Baxter, A. M. Rampey, G. T. Rushton, Y. Chen, and K. D. Shimizu, J. Chromatogr. B Analyt. Technol. Biomed. Life Sci. **804**, 141 (2004).
[6] I. A. Nicholls, Chem. Lett. ■, 1035 (1995).
[7] I. A. Nicholls, K. Adbo, H. S. Andersson, P. O. Andersson, J. Ankarloo, J. Hedin-Dahlstrom, P. Jokela, J. G. Karlsson, L. Olofsson, J. Rosengren, S. Shoravi, J. Svenson, and S. Wikman, Anal. Chim. Acta **435**, 9 (2001).
[8] B. Sellergren, M. Lepisto, and K. Mosbach, J. Am. Chem. Soc. **110**, 5853 (1988).
[9] H. S. Andersson, A. C. KochSchmidt, S. Ohlson, and K. Mosbach, J. Mol. Recognit. **9**, 675 (1996).
[10] M. J. Whitcombe, L. Martin, and E. N. Vulfson, Chromatographia **47**, 457 (1998).
[11] I. Chianella, M. Lotierzo, S. A. Piletsky, I. E. Tothill, B. N. Chen, K. Karim, and A. P. F. Turner, Anal. Chem. **74**, 1288 (2002).
[12] K. Karim, F. Breton, R. Rouillon, E. V. Piletska, A. Guerreiro, I. Chianella, and S. A. Piletsky, Adv. Drug Delivery Rev. **57**, 1795 (2005).
[13] S. Srebnik and O. Lev, J. Chem. Phys. **116**, 10967 (2002).
[14] S. Srebnik, Chem. Mater. **16**, 883 (2004).
[15] I. Yungerman and S. Srebnik, Chem. Mater. **18**, 657 (2006).
[16] X. Y. Wu, W. R. Carroll, and K. D. Shimizu, Chem. Mater. **20**, 4335 (2008).
[17] S. A. Piletsky, K. Karim, E. V. Piletska, C. J. Day, K. W. Freebairn, C. Legge, and A. P. F. Turner, Analyst (Cambridge, U.K.) **126**, 1826 (2001).
[18] I. Chianella, M. Lotierzo, S. A. Piletsky, I. E. Tothill, B. Chen, K. Karim, and A. P. F. Turner, Anal. Chem. **74**, 1288 (2002).
[19] I. Chianella, K. Karim, E. V. Piletska, C. Preston, and S. A. Piletsky, Anal. Chim. Acta **559**, 73 (2006).
[20] D. Pavel and J. Lagowski, Polymer **46**, 7543 (2005).
[21] D. Pavel, J. Lagowski, and C. J. Lepage, Polymer **47**, 8389 (2006).
[22] D. Pavel and J. Lagowski, Polymer **46**, 7528 (2005).
[23] S. Monti, C. Cappelli, S. Bronco, P. Giusti, and G. Ciardelli, Biosens. Bioelectron. **22**, 153 (2006).
[24] G. Ciardelli, C. Borrelli, D. Silvestri, C. Cristallini, N. Barbani, and P. Giusti, Biosens. Bioelectron. **21**, 2329 (2006).
[25] D. B. Henthorn and N. A. Peppas, Ind. Eng. Chem. Res. **46**, 6084 (2007).
[26] L. Sarkisov and C. Herdes, Langmuir (unpublished).
[27] P. R. Van Tassel, Phys. Rev. E **60**, R25 (1999).
[28] L. H. Zhang and P. R. Van Tassel, Mol. Phys. **98**, 1521 (2000).
[29] L. H. Zhang and P. R. Van Tassel, J. Chem. Phys. **112**, 3006 (2000).
[30] L. H. Zhang, S. Y. Cheng, and P. R. Van Tassel, Phys. Rev. E **6404**, 4 (2001).
[31] S. Cheng and P. R. Van Tassel, J. Chem. Phys. **114**, 4974 (2001).
[32] L. Sarkisov and P. R. Van Tassel, J. Phys. Chem. C **111**, 15726 (2007).
[33] L. Sarkisov and P. R. Van Tassel, J. Chem. Phys. **123**, (2005).
[34] R. Sporl and L. Sarkisov, *Characterization of Porous Solids VIII* (■, ■, 2009), p. 204.
[35] J. Kolafa and I. Nezbeda, Mol. Phys. **61**, 161 (1987).
[36] I. Nezbeda, J. Kolafa, and Y. V. Kalyuzhnyi, Mol. Phys. **68**, 143 (1989).
[37] R. Q. Snurr, A. T. Bell, and D. N. Theodorou, J. Phys. Chem. **97**, 13742 (1993).
[38] D. A. Spivak, Adv. Drug Delivery Rev. **57**, 1779 (2005).
[39] B. Sellergren, Macromol. Chem. Phys. **190**, 2703 (1989).

AUTHOR QUERIES — 056921JCP

#1   Au: Please supply authors initial and volume in Ref. 1.
#2   Au: Please supply volume number in Ref. 6.
#3   Au: Please update Ref. 26.
#4   CrossRef reports the author should be ″Zhang, Paul R. Van Tassel″ not ″Zhang″ in the reference 28 ″Zhang, Van Tassel, 2000″.
#5   Au: Please update volume, page, year for Ref. 30
#6   Au: Please supply publisher and location in Ref. 34.